

# Light interception efficiency explained by two simple variables: a test using a diversity of small- to medium-sized woody plants

R. A. Duursma<sup>1</sup>, D. S. Falster<sup>2</sup>, F. Valladares<sup>3</sup>, F. J. Sterck<sup>4</sup>, R. W. Pearcy<sup>5</sup>, C. H. Lusk<sup>6</sup>, K. M. Sendall<sup>2,7</sup>, M. Nordenstahl<sup>2</sup>, N. C. Houter<sup>8</sup>, B. J. Atwell<sup>2</sup>, N. Kelly<sup>9</sup>, J. W. G. Kelly<sup>2</sup>, M. Liberloo<sup>10</sup>, D. T. Tissue<sup>1</sup>, B. E. Medlyn<sup>2</sup> and D. S. Ellsworth<sup>1</sup>

<sup>1</sup>Hawkesbury Institute for the Environment, University of Western Sydney, Locked Bag 1797, Penrith 2751, NSW, Australia; <sup>2</sup>Department of Biological Sciences, Macquarie University, North Ryde, NSW 2109, Australia; <sup>3</sup>Instituto de Recursos Naturales, CSIC IRN-CCMA-CSIC, Madrid, Spain; <sup>4</sup>Forest Ecology and Management Group, Wageningen University, PO Box 47, 6700 AA, Wageningen, the Netherlands; <sup>5</sup>Section of Evolution and Ecology, University of California, Davis, CA 95616, USA; <sup>6</sup>Department of Biological Sciences, The University of Waikato, Private Bag 3105, Hamilton 3204, New Zealand; <sup>7</sup>Department of Plant Biological Sciences, University of Minnesota, St Paul, MN 55108, USA; <sup>8</sup>Department of Plant Ecophysiology, Institute of Environmental Biology, Utrecht University, 3584CH, Utrecht, the Netherlands; <sup>9</sup>CSIRO Mathematics, Informatics and Statistics, Castray Esplanade, Hobart, TAS 7000, Australia; <sup>10</sup>Department of Biology, University of Antwerp, 2610 Wilrijk, Belgium

## Summary

Author for correspondence:  
R. A. Duursma  
Tel: +61 245701806  
Email: remkoduursma@gmail.com

Received: 25 July 2011  
Accepted: 26 September 2011

New Phytologist (2011)  
doi: 10.1111/j.1469-8137.2011.03943.x

**Key words:** leaf area index, light interception, plant allometry, plant architecture, radiative transfer model, three-dimensional digitizing.

- Plant light interception efficiency is a crucial determinant of carbon uptake by individual plants and by vegetation. Our aim was to identify whole-plant variables that summarize complex crown architecture, which can be used to predict light interception efficiency.
- We gathered the largest database of digitized plants to date (1831 plants of 124 species), and estimated a measure of light interception efficiency with a detailed three-dimensional model. Light interception efficiency was defined as the ratio of the hemispherically averaged displayed to total leaf area. A simple model was developed that uses only two variables, crown density (the ratio of leaf area to total crown surface area) and leaf dispersion (a measure of the degree of aggregation of leaves).
- The model explained 85% of variation in the observed light interception efficiency across the digitized plants. Both whole-plant variables varied across species, with differences in leaf dispersion related to leaf size. Within species, light interception efficiency decreased with total leaf number. This was a result of changes in leaf dispersion, while crown density remained constant.
- These results provide the basis for a more general understanding of the role of plant architecture in determining the efficiency of light harvesting.

## Introduction

The crown architecture of plants is highly diverse, but it remains unclear how this diversity affects light interception and growth across species. Leaf display depends on a multitude of morphological traits (Hallé *et al.*, 1978; Barthélémy & Caraglio, 2007; Valladares & Niinemets, 2007), but it is difficult to generalize how these traits influence the light interception efficiency of individual plants. Moreover, different crown traits may result in similar light interception efficiencies (light interception per unit leaf area), suggesting functional equivalence of different architectural layouts (Valladares *et al.*, 2002). In this paper, we develop a coherent theoretical framework that allows the diversity in crown architectures seen among individual plants to be compared, in terms of their light interception efficiency. As plant productivity over long time-scales is approximately proportional to intercepted light (Monteith, 1977; Cannell *et al.*, 1987), it is hoped

that such a framework can provide a basis for understanding differences in productivity between plants and vegetation types.

Although plants vary in a myriad of qualitative architectural properties, models predicting light interception typically focus on a small number of quantitative features of the canopy, such as total leaf area, leaf angle distribution, and leaf dispersion (clumped, random, or regular) (Campbell & Norman, 2000), as these can be reliably quantified for different species and vegetation types. The well-known Lambert–Beer model estimates light interception by horizontally homogeneous canopies, assuming that leaves are randomly distributed in space (Monsi & Saeki, 1953, 2005):

$$Q_{\text{int}} = Q_0(1 - e^{-kL}) \quad \text{Eqn 1}$$

$Q_{\text{int}}$ , intercepted photosynthetic photon flux density (PPFD);  $Q_0$ , incident PPFD above the canopy;  $L$ , the leaf area index;  $k$ , an extinction coefficient.) However, random leaf spacing is clearly a

poor assumption for most real canopies, where foliage is clumped at shoot and whole-plant levels. As a result, model errors can be very large (Baldocchi *et al.*, 1985; Whitehead *et al.*, 1990; Cescatti, 1998). For this reason, a leaf dispersion parameter is frequently introduced in Eqn 1 (Nilson, 1971; Ross, 1981). The leaf dispersion parameter is typically estimated from inversion of PPFD transmission measurements in canopies (Nilson, 1971; Cescatti & Zorer, 2003), and is rarely related to direct measurements of canopy structure. A notable exception is a shoot clumping parameter developed for conifers (Oker-Blom & Smolander, 1988; Stenberg, 1996), but it is not clear how this parameter could be applied to other plant architectures. To this end, Sinoquet *et al.* (2007) developed a method based on the spatial variance of foliage in tree crowns, but this method seems to be difficult to apply to field measurements. The lack of a simple operational method to account for grouping of foliage is thus limiting our ability to link canopy light interception to plant and canopy structure.

A few attempts have been made to provide simplified models that account for grouping of foliage at the whole-plant scale (Jackson & Palmer, 1979; Kucharik *et al.*, 1999; Chen *et al.*, 2008; Ni-Meister *et al.*, 2010). However, the resulting models are often complex, with many species-specific parameters that are time-consuming to obtain. Furthermore, available models do not provide estimates of light interception by individual plants, limiting their usage to stand-scale applications. Estimates of light interception on an individual plant level are needed in individual-based models of vegetation dynamics (e.g. Moorcroft *et al.*, 2001; Falster *et al.*, 2011). A different field of study has avoided simplification altogether by developing highly detailed three-dimensional plant models with spatially explicit representation of leaves and stems. These studies have provided valuable insights

into the details of plant architecture and how it affects plant performance in specific environments (see reviews by Valladares & Pearcy, 1999; Pearcy *et al.*, 2005; Vos *et al.*, 2010). However, detailed architecture studies are yet to discover which aspects of canopy structure most influence whole-plant light interception, in part because of the limited sample sizes that necessarily result when using such methods.

Generally speaking, plant crowns are defined by the number, size, shape, three-dimensional distribution and orientation of their leaves. Together, these variables determine the size of the crown, the arrangement of leaves inside the crown, and the average leaf overlap ('self-shading') when viewed from a given direction. We define light interception efficiency as the ratio of displayed (i.e. exposed) to total leaf area, averaged over the entire sky hemisphere ( $\overline{\text{STAR}}$ ) (Farque *et al.*, 2001; Delagrange *et al.*, 2006) (see Table 1 for a list of symbols).  $\overline{\text{STAR}}$  relates directly to the amount of diffuse radiation intercepted by the plant, which can play an important role in determining total carbon uptake (Ackerly & Bazzaz, 1995; Roderick *et al.*, 2001). Direct light interception also scales with the sunlit leaf area fraction (Campbell & Norman, 2000), which is probably correlated with  $\overline{\text{STAR}}$ . Simple indices of self-shading – such as  $\overline{\text{STAR}}$  – have also been shown to predict total carbon uptake. For example, comparing branches from 38 perennial species, Falster & Westoby (2003) found that > 90% of variation in whole-branch  $\text{CO}_2$  assimilation rate expressed per unit leaf area (excluding differences in leaf photosynthetic capacity) was accounted for by an index of self-shading.  $\overline{\text{STAR}}$  has also been used in other applications to rank light interception efficiency of whole plants (Delagrange *et al.*, 2006; Sinoquet *et al.*, 2007) and shoots (Niinemets *et al.*, 2005), suggesting that it provides a reliable indicator of plant performance.

**Table 1** Symbols, their definitions and units

| Symbol                   | Definition  | Units                      |
|--------------------------|---|----------------------------|
| $L$                      | Leaf area index   | $\text{m}^2 \text{m}^{-2}$ |
| $A_C$                    | Crown surface area – total surface area of 3D convex hull wrapped around the leaf cloud | $\text{m}^2$               |
| $A_L$                    | Total plant leaf area   | $\text{m}^2$               |
| $A_{D,\Omega}$           | Displayed leaf area from angle $\Omega$   | $\text{m}^2$               |
| $H_\Omega$               | Crown silhouette area from angle $\Omega$   | $\text{m}^2$               |
| $P_\Omega$               | Crown porosity from angle $\Omega$  | –                          |
| $\overline{A}_D$         | Displayed leaf area averaged over all angles  | $\text{m}^2$               |
| $a_L$                    | Mean leaf area of individual leaves   | $\text{m}^2$               |
| $N$                      | Total plant leaf number   | –                          |
| $K$                      | Leaf projection coefficient averaged over all viewing angles                            | $\text{m}^2 \text{m}^{-2}$ |
| $k$                      | Extinction coefficient for a homogenous canopy  | $\text{m}^2 \text{m}^{-2}$ |
| $k_\Omega$               | Leaf projection coefficient from angle $\Omega$   | $\text{m}^2 \text{m}^{-2}$ |
| $\overline{\text{STAR}}$ | Silhouette to total area ratio, averaged over all viewing angles                        | $\text{m}^2 \text{m}^{-2}$ |
| $\beta$                  | Leaf dispersion parameter   | –                          |
| $\varepsilon$            | Empirical coefficient   | –                          |
| $\phi$                   | Empirical coefficient   | –                          |
| $\Omega$                 | Viewing angle (elevation, azimuth pair)   | –                          |
| $f_\Omega$               | Weighting function for $A_{D,\Omega}$   | –                          |
| $\alpha$                 | Solar elevation   | $^\circ$                   |
| $O_5$                    | Observed average distance to five nearest leaves  | m                          |
| $E_5$                    | Expected average distance to five nearest leaves for a random distribution              | m                          |

As possible predictors of  $\overline{\text{STAR}}$ , we propose two simple whole-plant variables: crown density and leaf dispersion. These variables were selected based on a statistical model predicting shading within the crown, based on similar models independently developed by Sinoquet *et al.* (2007) and Duursma & Mäkelä (2007), but with a new leaf dispersion parameter. The model is derived (see the Materials and Methods section) by viewing the plant first from one direction, and estimating the leaf area displayed in that direction from the silhouette of the crown, the number of leaves, the mean leaf area, and the mean leaf angle. After making simplifying assumptions, this leads to an approximation for the average leaf area displayed in all directions:

$$\overline{\text{STAR}} = \frac{\phi A_C}{\beta^\varepsilon A_L} \left(1 - e^{-\frac{K\beta^\varepsilon A_L}{\phi A_C}}\right), \quad \text{Eqn 2}$$

( $A_L/A_C$ , the crown density (ratio of plant leaf area,  $A_L$ , to crown surface area,  $A_C$ );  $\beta$ , a leaf dispersion parameter;  $\varepsilon$  and  $\phi$ , empirical parameters.) The ‘extinction coefficient’  $K$  is constant because we integrate over the entire hemisphere (Stenberg, 2006) (see the Materials and Methods section). The crown surface area is defined as the total surface area of a crown, that is, the area of a sheet wrapped around the crown. It is calculated as the surface area of the three-dimensional shape constructed by joining all outlying points of the plant crown, so that the shape is convex (i.e. there are no indentations in the three-dimensional shape). The remarkable aspect of the approximation (Eqn 2) is that only two plant variables, crown density ( $A_L/A_C$ ) and leaf dispersion ( $\beta$ ), are needed to estimate  $\overline{\text{STAR}}$ , in addition to the two (constant) parameters. In this paper we test the hypothesis that, across plants of diverse architecture, size, and growth environments, variation in  $\overline{\text{STAR}}$  can be explained by crown density and leaf dispersion. To do so, we used a database of 1831 virtual plants, reconstructed from precise digitization of the position and orientation of leaves and stems of real plants, to estimate  $\overline{\text{STAR}}$  (cf. Farque *et al.*, 2001). We then compared these empirical estimates to those given by the simplified model. Finally, we tested the hypothesis that  $\overline{\text{STAR}}$  declines with increasing plant size for a given species (Farque *et al.*, 2001; Niinemets *et al.*, 2005; Delagrangé *et al.*, 2006; Sinoquet *et al.*, 2007), and whether this decline is related to changes in leaf dispersion or crown density.

## Materials and Methods

### Model of light interception efficiency

Here, we derive a model for the light interception efficiency of individual plants with optically black – that is, nonreflecting and nontransmitting – leaves. We first consider the general case of light intercepted from an arbitrary direction. We then outline an approximation for the average light interception efficiency. Our derivation is similar to that provided by Duursma & Mäkelä (2007) and Sinoquet *et al.* (2007).

Consider a plant with  $N$  leaves, each with area  $a_L$ , and total leaf area  $A_L = N \cdot a_L$ . First consider the case where the sun is in the sky at a fixed position  $\Omega$  (defined by zenith and azimuth angle). For a plant with optically black leaves, light interception is proportional to the leaf area displayed in the direction of  $\Omega$  ( $A_{D,\Omega}$ ) (Ross, 1981), otherwise known as the ‘silhouette area’. Displayed leaf area can then be written as:

$$A_{D,\Omega} = H_\Omega(1 - P_\Omega), \quad \text{Eqn 3}$$

$H_\Omega$ , the outline area of the whole crown when viewed from  $\Omega$ ;  $P_\Omega$ , the porosity of that outline (Sinoquet *et al.*, 2007).  $H_\Omega$  is calculated from a two-dimensional convex hull wrapped around the leaf cloud and typically depends on  $\Omega$  and the crown shape.  $P_\Omega$  is the fraction of the outline not obscured by leaves, or the probability that a solar ray passes through the crown. Note that the probability that a light ray is not intercepted by a single leaf facing in the direction of  $\Omega$  is  $1 - a_L/H_\Omega$ . The probability that a light ray passes through a crown of  $N$  randomly distributed leaves, each with an average projected area of  $k_\Omega \cdot a_L$  in the direction  $\Omega$ , is then

$$P_\Omega = \left(1 - \frac{k_\Omega a_L}{H_\Omega}\right)^N. \quad \text{Eqn 4}$$

This equation is similar to a binomial model employed by Nilson (1971), with the difference that this approach does not require estimates of the path length of solar rays in the crown, but instead uses the outline area of the crown ( $H_\Omega$ ; cf. Sinoquet *et al.*, 2007).

Taking the log of both sides and using the fact that  $(1 - \frac{x}{N})^N$  tends to  $e^{-x}$  for large  $N$ , Eqn 4 can be reorganized into a form similar to the familiar Lambert–Beer law (Monsi & Saeki, 1953, 2005):

$$1 - P_\Omega \approx 1 - e^{-\frac{k_\Omega A_L}{H_\Omega}} \quad \text{Eqn 5}$$

Substituting the result from Eqn 5 into Eqn 3 gives an expression for  $A_{D,\Omega}$ :

$$A_{D,\Omega} = H_\Omega \left(1 - e^{-\frac{k_\Omega A_L}{H_\Omega}}\right) \quad \text{Eqn 6}$$

Next, we derive an approximation for the hemispherically averaged  $A_D$ . By definition,  $A_D$  averaged over all angles  $\Omega$  is given by

$$\overline{A_D} = \int_\Omega A_{D,\Omega} f_\Omega d\Omega = \int_\Omega f_\Omega H_\Omega \left(1 - e^{-\frac{k_\Omega A_L}{H_\Omega}}\right) d\Omega \quad \text{Eqn 7}$$

Here,  $f_\Omega$  is a weighting function whose integral over  $\Omega$  sums to unity. The integral in Eqn 7 is difficult to solve, because all variables depend on  $\Omega$  in complex ways. We hypothesize that Eqn 7 can be approximated by using effective averages for  $H_\Omega$  and  $k_\Omega$ . This simplification yields

$$\overline{A_D} = \langle H \rangle \left( 1 - e^{-\frac{\langle K \rangle A_L}{\langle H \rangle}} \right) \quad \text{Eqn 8}$$

where the angled brackets denote an effective average. The result in Eqn 8 is not exact, and it can be shown that the error of this approximation depends, among other factors, on the covariance of  $K_\Omega$  and  $H_\Omega$  along different viewing angles  $\Omega$  (in other words, the degree to which  $K_\Omega$  and  $H_\Omega$  are correlated).

The model can be completed by using the fact that  $H_\Omega$  averaged over all viewing angles is related to the lateral surface area of the convex hull ( $A_C$ ) through one of Cauchy's theorems:

$$\overline{H} \equiv \int_{\Omega} f_{\Omega} H_{\Omega} d\Omega = \frac{1}{4} A_C, \quad \text{Eqn 9}$$

where  $f_{\Omega}$  is a uniform weighting function. This result is general, and does not depend on the actual shape of the crown, as long as it is convex (see Lang (1991) for more details, and the section 'Crown surface area and leaf dispersion' for more clarification of  $A_C$ ). While Cauchy's theorem was originally derived for a spherical integration, Eqn 9 still holds for a hemispherical integration because the silhouette area is the same when viewed from either direction.

Similarly, the mean leaf projection function,  $\overline{k} = \int f_{\Omega} k_{\Omega} d\Omega$ , is well approximated by a function that depends on the mean leaf angle (Sinoquet *et al.*, 2007), or if the weighting function is uniform (i.e. all angles have equal weight), it is equal to 0.5 (Stenberg, 2006). We replace  $\langle K \rangle$  in Eqn 8 with  $K$ , which could be a function of the leaf angle distribution (but we leave the exact dependence for a further study).

Next, we replace  $\langle H \rangle$  in Eqn 8 with  $\overline{H}$  from Eqn 9, and use an empirical parameter  $\phi$  in place of the  $\frac{1}{4}$  to account for the fact that this rearrangement is not exact. This yields the final result for  $\overline{A_D}$ :

$$\overline{A_D} = \phi A_C \left( 1 - e^{-\frac{KA_L}{\phi A_C}} \right) \quad \text{Eqn 10}$$

Light interception efficiency is defined here by the ratio of  $\overline{A_D}$  to total leaf area ( $A_L$ ), commonly known as  $\overline{\text{STAR}}$  ('silhouette to total area ratio'), that is,  $\frac{\overline{A_D}}{A_L}$ :

$$\overline{\text{STAR}} = \frac{\phi A_C}{A_L} \left( 1 - e^{-\frac{KA_L}{\phi A_C}} \right) \quad \text{Eqn 11}$$

The result in Eqn 11 follows from the assumption that leaves are randomly distributed within the crown envelope (Eqn 4). We introduce a simple modification to account for a more clumped or more regular leaf dispersion. We use a dispersion parameter,  $\beta$ , defined so that if  $\beta = 1$ , leaves are randomly distributed. If  $\beta < 1$ , leaves are more clumped, and for  $\beta > 1$  they are more regular. We multiply  $A_L$  in Eqn 11 by this dispersion parameter, and include an empirical exponent  $\varepsilon$  that is to be estimated from

data. The final result is Eqn 2. It should be stressed that the modification for nonrandom leaf dispersion is a heuristic solution, and does not follow rigorous derivations such as those provided by, for example, Nilson (1971). The purpose of this study was to find a simple useful model of  $\overline{\text{STAR}}$  that can be evaluated against measurements.

### Virtual plant material

We collected existing input files for the 3D model YPLANT (see the next paragraph in this section) from published and unpublished sources. These plants were usually digitized with a 3D magnetic device (see Percy *et al.*, 2011), or sometimes measured by hand. For each virtual plant, all spatial locations of leaves were measured, as well as their orientation (see Fig. 1 for examples of digitized plants). Leaf shape was determined by  $x, y$  coordinates of leaf margins of a representative leaf, but leaf size is allowed to vary within plants. Stem sections, and their diameters, were also included (with the exception of two subdatasets; see Supporting Information Table S1). The collection includes plants, from widely differing environments (understorey, glasshouse and plantation), of 124 different species from different taxonomic families, and from all across the globe (Valladares *et al.*, 2000, 2002, 2005; Falster & Westoby, 2003; Percy *et al.*, 2004; Lusk *et al.*, 2006, 2011; Reich *et al.*, 2009; and a number of unpublished studies; see Table S1 for more details). We excluded a few plants from our final analysis: plants with leaves that were folded across the midrib (Falster & Westoby, 2003) and plants with fewer than six leaves, in both cases because the leaf dispersion parameter could not be calculated correctly, leaving 1831 plants in the database. Species of two genera dominated the collection: *Psychotria* (644 plants of 19 species) and *Eucalyptus* (295 plants of five species). The rest of the collection had an average of nine individuals per species.

We used the 3D plant model YPLANT (Percy & Yang, 1996; Percy *et al.*, 2011) to estimate the amount of leaf area displayed in different directions ( $A_D$ ). YPLANT accounts for the detailed 3D distribution of leaf elements. Shading by stems was also accounted for (except in two of the data sets; see Table S1), but was only a small source of variation in  $A_D$  (not shown). YPLANT does not account for penumbral effects, but the penumbra does not affect total light interception (Stenberg, 1998). In YPLANT,  $A_D$  is calculated for the centroids of each of 160 sectors of the hemisphere, corresponding to eight classes of azimuth and 20 solar elevation ( $\alpha$ ) classes (Percy & Yang, 1996). We calculated a hemispherically averaged STAR from these individual estimates of  $A_D$ , by weighting each  $A_D$  by the relative area of each sector. First, we averaged STAR ( $A_D/A_L$ ) across all azimuth values for a given  $\alpha$ . We then weighted these  $\text{STAR}_{\alpha}$  values by the area of the zone (the area of a section of the hemisphere between  $\alpha_1$  and  $\alpha_2$ ). This area is proportional to  $\sin(\alpha_2) - \sin(\alpha_1)$ , where  $\alpha_2$  is the larger of the two angles that define the zone. This yielded an estimate of  $\overline{\text{STAR}}$  for each plant that is consistent with its use in the summary model. An alternative method to finding  $\overline{\text{STAR}}$  is provided by the VEGESTAR software package (Adam *et al.*, 2002).



**Fig. 1** Examples of three-dimensional (3D) digitized plants and their 3D convex hull.

### Crown surface area and leaf dispersion

In the derivation of Eqn 2, we used the fact that the average two-dimensional projected area of any convex three-dimensional shape is a quarter of its surface area (Eqn 9); a famous theorem by Cauchy (Lang, 1991). For example, for a sphere, the projection is a circle (area =  $\pi r^2$ ), which is one quarter of the total spherical surface area (area =  $4\pi r^2$ ). While this theorem is useful in determining canopy extinction coefficients (Stenberg, 2006), it also implies that the correct definition of crown size with respect to light interception is that defined by its three-dimensional convex hull which contains all the leaves (Duursma & Mäkelä, 2007). We used the *quickhull* algorithm (Barber *et al.*, 1996), in the *geometry* package in R (R Development Core Team, 2010) to find the convex hull (and its surface area) spanning the leaves, using all coordinates of the leaf edges. This algorithm finds the smallest set of  $x$ ,  $y$ ,  $z$  points that defines the convex hull, that is, the polyhedral surface that contains all other points, and is convex (see Fig. 1 for examples of convex hulls).

As an index of leaf dispersion, we used a nearest-neighbour approach to quantify deviation from a random distribution of leaf positions within the convex hull. For each leaf, we calculated the mean distance between the midpoint of that leaf to the midpoint of the five nearest leaves. This mean distance was calculated for each leaf, and averaged over all leaves. This yielded the observed mean distance to the five nearest leaves ( $O_5$ ). We compared  $O_5$  to the expected distance if the leaf locations were completely random within the convex hull ( $E_5$ ) (see Fig. 3a). This expected value was calculated numerically (for 10 replicates), for a square box with the same volume and number of leaves as the plant crown to account for edge effects. This edge-effect-corrected  $E_5$  was not much different from an estimate where we did not account for the edge effect (Fig. 3a), so more precise methods that account for the actual shape of the plant crown were not applied. The leaf dispersion was defined as  $O_5/E_5$ . Other choices for the number of neighbouring leaves were also tested (between two and 25), without large effects on the goodness of fit or any other of the main results. Values of unity indicate a random distribution, while values of less than unity

indicate a more clumped distribution, and values larger than unity a distribution that is more regular than random.

Both the crown surface area ( $A_C$ ) and leaf dispersion ( $\beta$ ) were estimated for the digitized plants, but it is possible to measure both variables on plants in the field. There is a close linear correlation between  $A_C$  and the product of crown width and length, with the constant of proportionality depending on the crown shape (e.g. cone vs ellipse). Both crown width and length are easily measured in the field, and can thus be used to provide estimates of  $A_C$  (Duursma *et al.*, 2010). For  $\beta$ , it is necessary to measure the distance to the five nearest leaves ( $O_5$ ), whereas the expected distance to the five nearest leaves ( $E_5$ ) is readily obtained from simulation (using the R package *YpTools*; see Pearcy *et al.*, 2011). For our virtual plants, we measured  $O_5$  for all leaves, but sufficiently accurate estimates can be obtained based on a random sample of leaves. A random table may be used for small plants, where all leaves can be assigned a number, or for larger plants a stratified sampling strategy may be employed (by first selecting branches at random, and then leaves within branches).

### Data analysis

The two variables in the model ( $A_L/A_C$  and  $\beta$ ) were determined for each plant. The  $K$  parameter was set to 0.5, and the remaining two empirical parameters in Eqn 1,  $\phi$  and  $\varepsilon$ , were estimated by nonlinear regression (using the 'nls' function in R), that is, the two empirical parameters are the same for all plants. The model  $R^2$  was then calculated as  $1 - \sigma_R^2/\sigma_Y^2$ , where  $\sigma_R^2$  is the variance of the model residual, and  $\sigma_Y^2$  is the variance of the dependent variable across single plants ( $\overline{STAR}$ ) (Kvålseth, 1985). We analysed the residuals for patterns with a number of plant structure variables, such as  $A_L$ ,  $A_C$ ,  $\beta$ , number of leaves, and crown shape.

As with any data-pooling exercise, our data set is potentially confounded by multiple factors, such as experimental setting, growth environment, and unmeasured traits conserved within genera, within families or at a higher taxonomic level. We adopted two approaches to determine whether taking account of clade membership improves predictions of light interception efficiency. First, we refitted the model by family, to determine whether this resulted in divergent parameter sets. Secondly, we

used a linear mixed-effects model to partition the residual variance into division (Angiosperm or Conifer), family, and species (using nested random effects), and the light environment (shaded, intermediate or exposed, using a fixed effect) (with the *nlme* package in R).

The scaling of  $A_L$  with  $A_C$ , and the correlation between  $\overline{STAR}$  and total leaf number were tested with standardized major axis (SMA) following Warton *et al.* (2006), for each species separately, using a subset of the data where individual species had at least five replicates.

### Results

The data set included plants with a wide range in leaf area and displayed area (Fig. 2a), and a wide range in  $\overline{STAR}$  as estimated by the YPLANT model (Fig. 2b). Note that the limit value of  $\overline{STAR}$  (calculated for the whole hemisphere) is 0.5, obtained when there is no overlap between leaves. However, plants with more than one leaf cannot actually achieve this value when  $\overline{STAR}$  is calculated for the whole hemisphere. As indicated by the measure of leaf dispersion ( $\beta$ ), 608 of the 1831 plants showed a clumped arrangement in crowns (Fig. 3), while 460 plants tended to a more regular display, leaving 763 plants where the leaf dispersion was not significantly different from a random distribution.

The simple model (Eqn 2) incorporating both crown density and leaf dispersion explained 85% of the variation in  $\overline{STAR}$  across the 1831 virtual plants (Figs 4, 5). As shown in Fig. 5,  $\overline{STAR}$  declined consistently with increasing  $A_L/A_C$  at a given value of  $\beta$ , and increased with  $\beta$  at a given value of  $A_L/A_C$ . By itself,  $A_L/A_C$  explained only 43% of the variation in  $\overline{STAR}$  (by refitting the model after setting  $\beta$  to a constant value), and  $\beta$  explained only 33% (see Table 2 for details). We performed a residual analysis to determine if variables not included in the model explained additional variation in  $\overline{STAR}$ . This analysis did not reveal any systematic over- or underestimation related to the leaf angle distribution or total plant leaf area, and only a weak relationship with crown shape (giving a slight overestimation for flat crowns) (Fig. S1). It is not surprising that we found no correlation between the residuals and the leaf angle distribution, as we

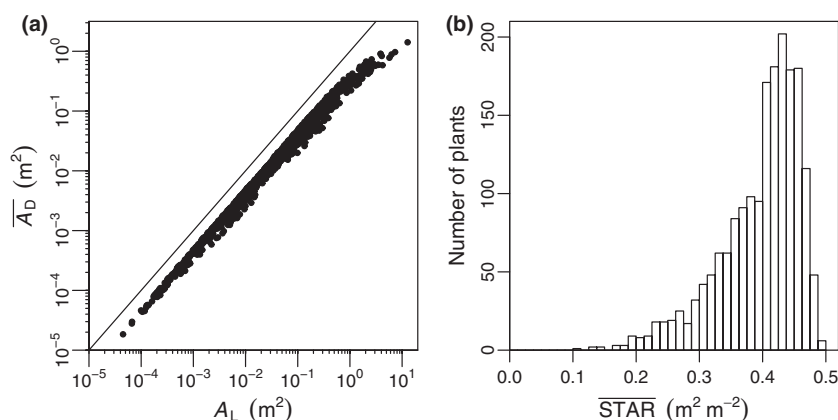


**Fig. 2** (a) Displayed leaf area ( $A_D$ ) (hemispherically averaged) as a function of total plant leaf area ( $A_L$ ). The solid line is a 1 : 1 line. Each point is a plant (1831 plants). (b) Frequency plot of  $\overline{STAR}$  values for the whole data set, where  $\overline{STAR}$  is defined as  $\frac{A_D}{A_C}$ . The theoretical maximum  $\overline{STAR}$  is 0.5.

**Fig. 3** (a) Illustration of the two components of the leaf dispersion parameter. The mean distance to five nearest leaves is a decreasing function of the leaf number density (number of leaves per unit crown volume). For a random distribution, these mean distances ( $E_5$ ) were obtained by numerical simulation. The thick line indicates the mean, and the thin lines the 5 and 95% quantiles; the variation in  $E_5$  at a given leaf number density is the result of edge effects and, to a lesser extent, stochastic effects of the numerical simulation. For real plants (grey circles), the mean distance to five nearest leaves ( $O_5$ ) was calculated for each leaf, and averaged. The leaf dispersion parameter ( $\beta$ ) is calculated as  $O_5/E_5$ , so that  $\beta < 1$  indicates a clumped distribution, and  $\beta > 1$  a more uniform distribution. (b) Histogram of the leaf dispersion parameter as estimated for all plants in the data set.

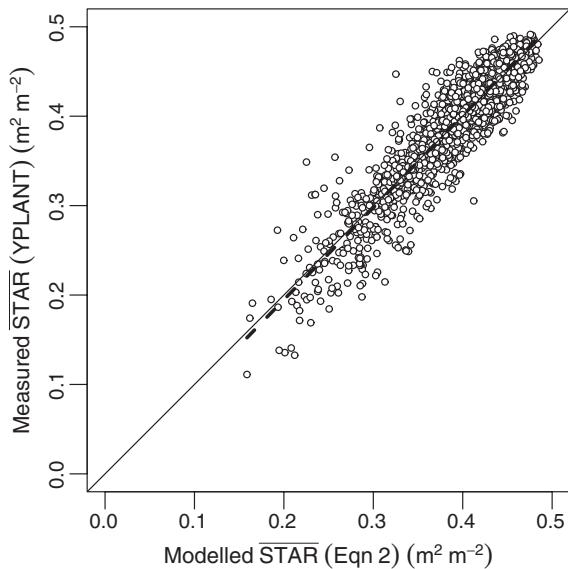
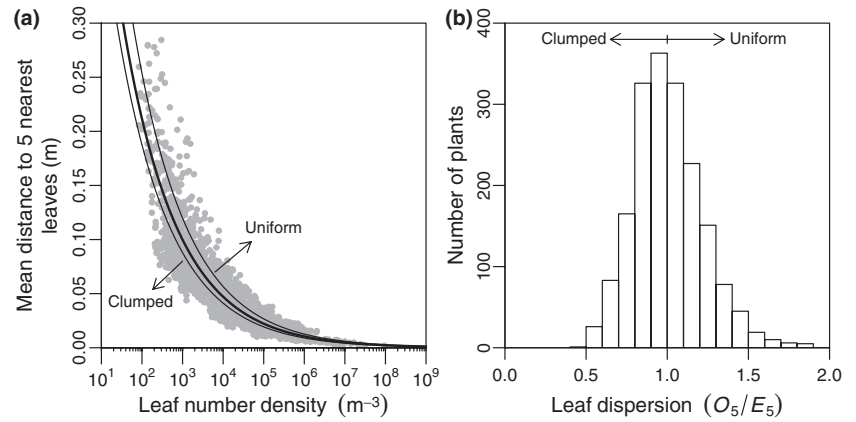


**Fig. 4** Measured  $\overline{\text{STAR}}$  (silhouette to total area ratio, averaged over all viewing angles) of the virtual plants (estimated with YPLANT) compared against the modelled estimates from the summary model (Eqn 2). The dashed line is a regression line ( $y = -0.011 + 1.03x$ ,  $R^2 = 0.848$ , RMSE, root mean squared error = 0.025). Each point is a plant (1831 plants).

used the hemispherically averaged  $\overline{\text{STAR}}$  in our model, but a correlation might arise if the leaf angle distribution was related to unmeasured traits that affect  $\overline{\text{STAR}}$ .

Variation between and within species dwarfed the influences of family and division membership on differences in light interception efficiency. The model performed equally well – or better – when fitted to each plant family separately, with one exception (Myrtaceae) (Fig. S2). However, the estimated parameter values ( $\phi$  and  $\varepsilon$ ) did not vary greatly between families. These results show that the excellent fit of the model to the full data set was not confounded by taxonomic relatedness, and that the same model can predict  $\overline{\text{STAR}}$  for a variety of taxa. However, there was some indication of taxa-specific effects that are not accounted for in the simple model. Partitioning of the residual variance from the full model showed that 14.1% was related to division (Gymnosperm or Angiosperm), 3.7% to family, 36.9% to

species, and the remaining 45.6% to individual within species. Thus, an additional 8.25% of total variance in  $\overline{\text{STAR}}$  (55% of residual variance) could be attributed to species, family, or division, in addition to the 85% of total variance already accounted for by crown density and leaf dispersion.

Within species, the leaf dispersion parameter was closely related to total leaf number ( $N$ ). There was a strong tendency for plants with more leaves to exhibit a more clumped leaf dispersion (Fig. 6a). This observed correlation was directly related to  $N$ , because at a given  $A_L$ ,  $\beta$  increased with mean leaf size (i.e. plants with smaller leaves have more clumped foliage) (Fig. 6b). Secondly, at a given leaf size, the dispersion parameter ( $\beta$ ) decreased with  $A_L$  (i.e. larger plants had more clumped foliage) (Fig. 6c). These two patterns are confounded when leaf dispersion is plotted against either leaf size or leaf area, because larger leaved species tended to have greater total area in our data set. To illustrate this, we fit a simple regression model to leaf dispersion ( $\beta$ ) as a function of total plant leaf area ( $A_L$ ) and mean leaf size ( $a_L$ ), as  $\beta = bA_L^c \times a_L^d$  (see Fig. 6), which can also be rearranged as  $\beta = aN^c \times a_L^{(c+d)}$ . Because  $c \approx -0.15$  and  $d \approx 0.15$ , the leaf size component cancels, leaving a dependence of  $\beta$  on number of leaves (with exponent  $\approx -0.15$ ).

Finally, we tested the hypothesis that  $\overline{\text{STAR}}$  declines with plant size. We found a strong relationship between  $\overline{\text{STAR}}$  and total leaf number ( $N$ ) (Fig. 7a). Out of the 65 species in the data set that had more than five replicates, 50 showed a significant negative correlation between  $\overline{\text{STAR}}$  and  $N$ . To assess whether this decrease in  $\overline{\text{STAR}}$  with increasing  $N$  was attributable to leaf dispersion (Fig. 6) or crown density ( $A_L/A_C$ ), we tested for size-related trends in  $A_L/A_C$  by assessing the scaling of  $A_L$  as  $A_L = aA_C^b$  (Fig. 7b). If the exponent  $b > 1$ , this would result in an increase in  $A_L/A_C$  with  $A_C$ , and would lead to decreased light interception efficiency with increasing crown size. Out of the 65 species, 38 showed an exponent not significantly different from unity (the mean exponent estimated by SMA was 1.05; SD = 0.25). For the remainder of the data set, 18 species had an exponent  $> 1$ , and only nine had an exponent  $< 1$ . There is, then, no general evidence that  $A_L/A_C$  increased with plant size in this data set, and the decrease in  $\overline{\text{STAR}}$  with  $N$  is entirely attributable to a more clumped leaf dispersion in larger plants.

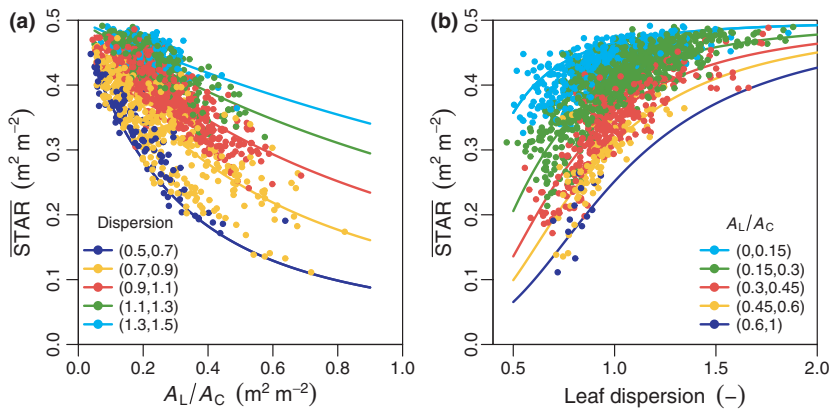


**Fig. 5** Measured and modelled  $\overline{STAR}$  as a function of crown density and leaf dispersion. (a)  $\overline{STAR}$  (silhouette to total area ratio, averaged over all viewing angles) as related to the ratio of leaf area ( $A_L$ ) to crown surface area ( $A_C$ ), in five bins of the leaf dispersion parameter (see key for the bin ranges). Lines are predictions from the simple nonlinear model (Eqn 2), using  $A_L/A_C$  and the midpoint of each of the dispersion bins (and two empirical parameters; see Table 2). Each point is a plant (1831 plants). (b) Same as (a), but  $\overline{STAR}$  is plotted against leaf dispersion in five bins of crown density ( $A_L/A_C$ ).

**Table 2** Diagnostics of the nonlinear regression fit of the simple model of  $\overline{STAR}$  (Eqn 2) to the whole data set

| Model           | $R^2$ | RMSE (m <sup>2</sup> m <sup>-2</sup> ) |
|-----------------|-------|--|
| Full model      | 0.847 | 0.0251                                 |
| $A_L/A_C$ only  | 0.426 | 0.0486                                 |
| Dispersion only | 0.324 | 0.0527                                 |

Parameter values were  $\phi = 0.254$  (SE = 0.0019), and  $\varepsilon = -2.28$  (SE = 0.034), with  $K$  set to 0.5. Shown are the  $R^2$  and RMSE (root mean squared error) for the full model, and for two simplified models where dispersion was excluded (' $A_L/A_C$  only') or  $A_L/A_C$  was excluded from the model fit ('dispersion only') (and instead set to the average value for the whole data set).

## Discussion

We found that two simple variables, summarizing the display of leaves in plant crowns, explained most of the variation in plant light interception efficiency ( $\overline{STAR}$ ) for 1831 plants of 124 species across a variety of environments. The first variable, crown density, is given by the ratio of leaf area to crown hull surface area. The second variable, leaf dispersion, describes the arrangement of leaves inside the crown. Moreover, our model provides a robust framework for ranking individual plants in terms of  $\overline{STAR}$ , and thus for understanding trade-offs in structure and function of plant crowns. Carbon uptake is closely linked to plant light interception; therefore, our results will also help improve ecosystem models aimed at quantifying plant structure and productivity.

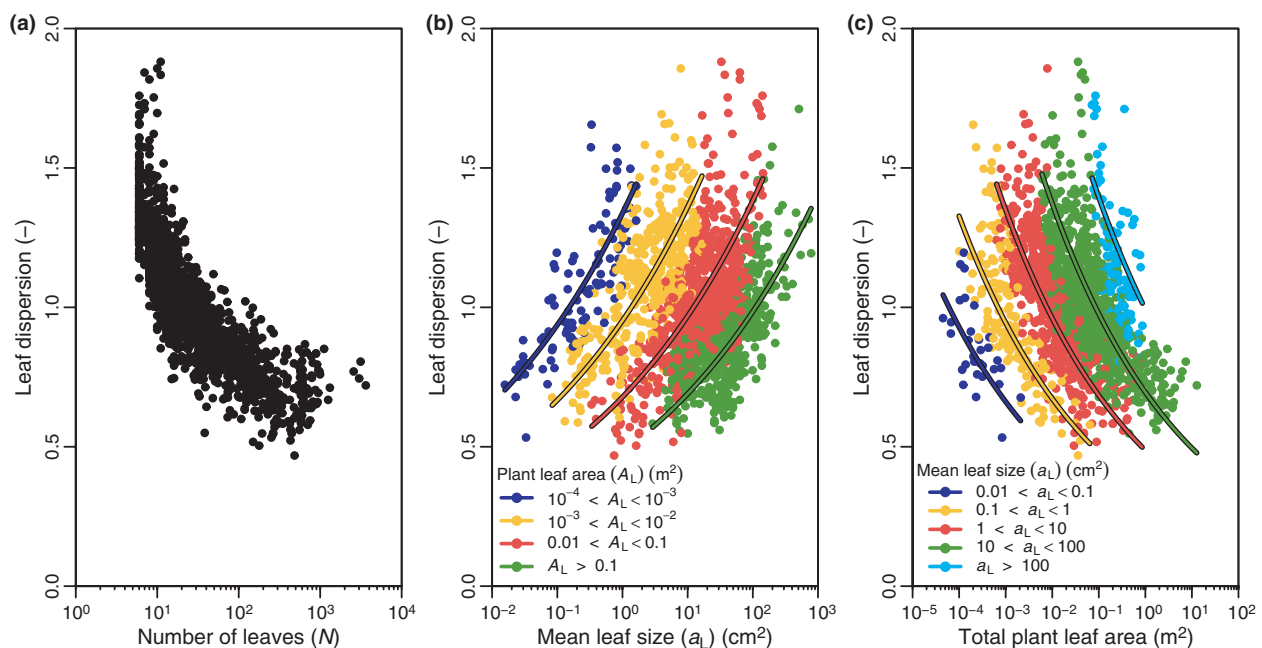


**Fig. 6** Leaf dispersion is related to number of leaves per plant ( $N$ ), total plant leaf area ( $A_L$ ) and mean leaf size ( $a_L$ ). Leaf dispersion (a) decreases markedly with  $N$ , and (b) increases with  $a_L$  at a given total plant leaf area ( $A_L$ ), and (c) decreases with  $A_L$  at a given  $a_L$ . The solid black curves are predictions from a regression model of the form:  $\beta = b \cdot A_L^c \cdot a_L^d$ , fitted to the entire data set by linear regression after log-transformation ( $R^2 = 0.71$ ,  $b = 0.39$ ,  $c = -0.15$ ,  $d = 0.15$ ; interaction not significant).

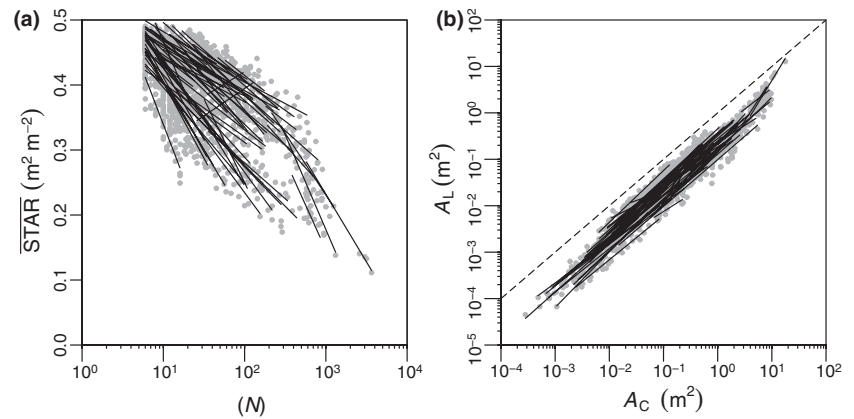


**Fig. 7** (a) The relationship between total leaf number ( $N$ ) and  $\overline{STAR}$  (silhouette to total area ratio, averaged over all viewing angles) for a subset of the data set, including 65 species with at least five replicates (1647 plants). The lines are standardized major axis fits to each species separately. (b) Scaling of total plant leaf area ( $A_L$ ) with crown surface area ( $A_C$ ) for the same data set as in (a). The lines are standardized major axis fits to each species separately. The dashed line is a 1 : 1 line.

### Determinants of light interception efficiency

Although several other traits have been shown to affect plant light interception (see review by Valladares & Niinemets, 2007), our study implies that these variables are either summarized by the two simple variables used here or play a relatively small part in determining light interception efficiency. For example, phyllotaxy (arrangement of leaves on plant stems) (Brites & Valladares, 2005), petiole twisting (Gálvez & Pearcy, 2003), and petiole lengthening (Takenaka, 1994) will affect the leaf dispersion parameter, and the crown density if crown size is affected. The crown shape (length to width ratio) affects crown density, unless crown hull surface area is held constant – explaining at least some of the theoretical relationships between crown shape and light interception (see Duursma & Mäkelä, 2007). We expect that previously published interspecific comparisons in  $\overline{STAR}$  (Valladares *et al.*, 2002; Pearcy *et al.*, 2004) could be partly explained in terms of crown density and leaf dispersion (see also Planchais & Sinoquet, 1998; Cescatti & Zorer, 2003; Massonnet *et al.*, 2008). Therefore, our analysis provides a more robust mechanistic framework for interpreting interspecific comparisons.

We found that the clumping of leaves within crowns increased with increasing plant size and with decreasing leaf size. A previous study argued that the centroids of smaller leaves are necessarily closer to plant stems and to each other (Falster & Westoby, 2003), leading to a more clumped distribution. Our results support this interpretation. The connection between clumping and plant size, however, is less widely recognized. A more clumped distribution is less costly in terms of supporting biomass as plants grow larger, because fewer branches are needed to support a given total leaf area when leaves are closer together. Thus, increased clumping may be favoured, despite the reductions in light interception. Similarly, gradual shedding of leaves inside crowns leads to a more clumped distribution because newer leaves are borne at the tips of branches. In any case, this novel finding points to a connection between crown structure and function that is yet to be explored.

In a simplistic viewpoint, plants with high  $\overline{STAR}$  should outperform those with lower  $\overline{STAR}$  because they intercept more light per unit leaf area, which would lead to higher whole-plant

carbon uptake rates. Nonetheless, we observed a wide range in  $\overline{STAR}$  (Fig. 2b), even among co-occurring plants. We found that  $\overline{STAR}$  declined with increasing total leaf number for the majority of the species in our data set, and that this decline was attributable to a more clumped leaf dispersion in larger plants (Figs 6, 7a), while crown density ( $A_L/A_C$ ) remained roughly constant (Fig. 7b). Other studies have also found a decline in  $\overline{STAR}$  (or related measures) with increasing plant size. Niinemets *et al.* (2005) found decreased light interception efficiency of shoots in *Agathis australis* with increasing tree size, while several other studies (Farque *et al.*, 2001; Delagrange *et al.*, 2006; Sinoquet *et al.*, 2007; Lusk *et al.*, 2011) have found a decrease in  $\overline{STAR}$  with increasing  $A_L$  in a variety of species. Our results generalize and extend these previous findings.

Variation in  $\overline{STAR}$  of plants grown in a common light environment can probably be understood through a cost–benefit analysis of plant architecture (cf. Küppers, 1989; Sterck & Schieving, 2007): maintaining a high light interception efficiency incurs a substantial cost via the construction and maintenance of the woody structures needed for support and water supply. Taking into account the balance between biomass cost and gain from photosynthesis, Pearcy *et al.* (2005) showed that the optimum internode length (and therefore crown density) was shorter than that required for maximal light interception. Similarly, others (Mäkelä & Sievänen, 1992; Duursma *et al.*, 2010) have found that it is beneficial for plants to slightly decrease  $\overline{STAR}$  (by increasing  $A_L/A_C$ ) with increasing plant size because the construction cost increases more than the benefit from higher light interception per unit leaf area. However, here we found approximately isometric scaling between  $A_L$  and  $A_C$ , which would lead to a roughly constant  $A_L/A_C$  with plant size (Fig. 7b). Taken together, these results provide a link between light interception efficiency and the cost for leaf display as a plant grows, because total plant woody biomass scales closely with  $A_C$  (Mäkelä, 1997; Valentine & Mäkelä, 2005; Duursma *et al.*, 2010). The strong influence of leaf dispersion on  $\overline{STAR}$  found in this study suggests that a cost–benefit analysis of leaf dispersion is worth investigating.

We have so far ignored variation in leaf angle, although leaf angle distribution affects the function of real plants (Valladares & Pearcy, 1998; Falster & Westoby, 2003). Benefits of steep leaf

angles include avoidance of photo-damage caused by excess sunlight in hot midday conditions (Valladares *et al.*, 2005), and avoidance of high leaf temperatures (Valiente-Banuet *et al.*, 2010). The model for  $\overline{\text{STAR}}$  was based on the assumption that diffuse skylight has no angular dependence, so that  $K = 0.5$  for any leaf angle distribution. It has previously been shown that  $K$  can be a simple function of the mean leaf angle if light does have a strong angular dependence (Sinoquet *et al.*, 2007). Such dependence will be stronger for plants growing beneath small canopy gaps. Clearly, the trade-off between diffuse and direct light will affect plant architecture, as well as the correct definition of  $\overline{\text{STAR}}$ . In support of the importance of diffuse light, Ackerly & Bazzaz (1995) found that the leaf orientation of seedlings in the field was influenced by the hemispherical distribution of diffuse (rather than direct) light sources.

### Relation to other radiative transfer models

Radiative transfer modelling in plant canopies has shown that complex canopy structure can be summarized with measures of canopy density (leaf area per unit volume) and a leaf dispersion parameter (Nilson, 1971; Ross, 1981). Our approach is similar to an aggregated turbid medium model (Ross, 1981) but applied to single isolated plant crowns instead of horizontally extended canopies. A similar approach was used by Cescatti & Zorer (2003) and Niinemets *et al.* (2005) for conifer shoots, but their approach requires information on the path length of rays through the shoot envelope. The novelty of our approach is that, instead of testing the complex integral of the displayed leaf area over all viewing angles directly against measurements (Eqn 7), we hypothesized a simple approximation that yields a compact model. The final model is essentially equivalent to that proposed by Sinoquet *et al.* (2007) and Duursma & Mäkelä (2007) but with a different form of the leaf dispersion parameter. Our nearest-neighbour approach to the leaf dispersion parameter is novel; previous approaches have used the variance of the contact number (Nilson, 1971), the variance in leaf area density within crown envelopes (Sinoquet *et al.*, 2005), and  $\overline{\text{STAR}}$  of conifer shoots (Stenberg, 1996).

### Relation to stand-level models of light interception

The importance of leaf dispersion (i.e. clumped vs regular leaf dispersion) has long been recognized (Nilson, 1971; Baldocchi *et al.*, 1985; Whitehead *et al.*, 1990) but some ecosystem models continue to assume that foliage is randomly distributed. Nilson (1999) showed that the problem of canopy transmission in heterogeneous canopies can be simplified when separating within-plant from between-plant shading. Canopy transmission is then a function of self-shading, which is a function of crown density and leaf dispersion as we have shown, and the spatial distribution of neighbouring plants. In the simplest case of identical plants that are randomly distributed in space, the fraction of light intercepted by a canopy ( $f_{\text{APAR}}$ ) approximately follows Lambert–Beer's law (Eqn 1) with the extinction coefficient depending on  $\overline{\text{STAR}}$  of the individual plants (see Methods S1):

$$f_{\text{APAR}} \approx 1 - e^{-\overline{\text{STAR}} \cdot L} \quad \text{Eqn 12}$$

The interpretation of this equation is that, at a given total leaf area index  $L$ , a canopy consisting of crowns with a low  $\overline{\text{STAR}}$  will intercept a lower fraction of available light than a canopy consisting of plants with high  $\overline{\text{STAR}}$ . Adjustments for nonrandom distribution of plants can also be introduced (Nilson, 1999). It would be worthwhile to test this equation for real stands, or against a detailed canopy-scale model that takes into account grouping of foliage in tree crowns.

The simple canopy-scale model of light interception (Eqn 12) used plant  $\overline{\text{STAR}}$ , which describes light interception from all angles. However, for individual plants in canopies, light can be strongly directional. Duursma & Mäkelä (2007) compared this model to a detailed stand-level model of light interception, and found good agreement, but the leaf angle was kept constant in those simulations. For our data set, we have also calculated  $\overline{\text{STAR}}$  averaged over a  $30^\circ$  canopy gap ( $\overline{\text{STAR}}_{30}$ ) centered at the zenith (results not shown). Our model for  $\overline{\text{STAR}}$  explained only 52% of the variance in  $\overline{\text{STAR}}_{30}$ , but when a function of leaf angle was added to the model (in place of  $K$  in Eqn 2), the  $R^2$  increased to 81%. The effect of crown shape was also significant, but of minor importance compared with the strong effect of leaf angle. A further generalization of the simple model presented here to plants growing under gaps or in stands of plants will be the subject of a future contribution.

### Conclusion

We identified two simple variables that together explain 85% of variation in silhouette-to-area ratio of foliage ( $\overline{\text{STAR}}$ ), a measure of light interception efficiency, across a diverse collection of plants. We think it is feasible to develop methods for field sampling of both these variables (crown density and leaf dispersion), potentially obviating the need for detailed models to predict light interception efficiency if a basic index of light interception efficiency is warranted. A simple model of  $\overline{\text{STAR}}$  that incorporates these two variables can be readily incorporated in canopy models (cf. Duursma & Mäkelä, 2007). We found that  $\overline{\text{STAR}}$  was negatively correlated with total plant leaf number for most of the species in the data set, as a result of a more clumped leaf dispersion for larger plants. These results allow a more general interpretation of the wide diversity in plant architecture, and its connection to plant and canopy function. We thus provide a new framework for understanding how the diversity found in crown architecture contributes to plant convergence or divergence in light interception efficiency, both within and across plant communities.

### Acknowledgements

B.E.M. and D.S.E. acknowledge the support of the Australian Research Council (ARC) (grant DP0881221), and D.T.T. received support from ARC grant DP0879531. R.A.D. was partly supported by a NSW Government Climate Action Grant (NSW T07/CAG/016). B.J.A. thanks Aderajew Haddis for assistance with collection of eucalypt data.

## References

- Ackerly DD, Bazzaz FA. 1995. Seedling crown orientation and interception of diffuse radiation in tropical forest gaps. *Ecology* 76: 1134–1146.
- Adam B, Donès N, Sinoquet H. 2002. *VegeSTAR – software to compute light interception and canopy photosynthesis from images of 3D digitised plants, Version 3.0*. Clermont-Ferrand, France: UMR PIAF INRA-UBP.
- Baldocchi DD, Hutchison BA, Matt DR, McMillen RT. 1985. Canopy radiative transfer models for spherical and known leaf inclination angle distributions: a test in an oak-hickory forest. *Journal of Applied Ecology* 22: 539–555.
- Barber CB, Dobkin DP, Huhdanpaa H. 1996. The quickhull algorithm for convex hulls. *ACM Transactions on Mathematical Software (TOMS)* 22: 469–483.
- Barthélémy D, Caraglio Y. 2007. Plant architecture: a dynamic, multilevel and comprehensive approach to plant form, structure and ontogeny. *Annals of Botany* 99: 375–407.
- Brites D, Valladares F. 2005. Implications of opposite phyllotaxis for light interception efficiency of Mediterranean woody plants. *Trees – Structure and Function* 19: 671–679.
- Campbell GS, Norman JM. 2000. *An introduction to environmental biophysics*. New York, NY, USA: Springer Verlag.
- Cannell MGR, Milne R, Sheppard LJ, Unsworth MH. 1987. Radiation interception and productivity of willow. *Journal of Applied Ecology* 24: 261–278.
- Cescatti A. 1998. Effects of needle clumping in shoots and crowns on the radiative regime of a Norway spruce canopy. *Annales Des Sciences Forestières* 55: 89–102.
- Cescatti A, Zorer R. 2003. Structural acclimation and radiation regime of silver fir (*Abies alba* Mill.) shoots along a light gradient. *Plant, Cell & Environment* 26: 429–442.
- Chen Q, Baldocchi D, Gong P, Dawson T. 2008. Modeling radiation and photosynthesis of a heterogeneous savanna woodland landscape with a hierarchy of model complexities. *Agricultural and Forest Meteorology* 148: 1005–1020.
- Delagrange S, Montpied P, Dreyer E, Messier C, Sinoquet H. 2006. Does shade improve light interception efficiency? A comparison among seedlings from shade-tolerant and -intolerant temperate deciduous tree species. *New Phytologist* 172: 293–304.
- Duursma RA, Mäkelä A. 2007. Summary models for light interception and light-use efficiency of non-homogeneous canopies. *Tree Physiology* 27: 859–870.
- Duursma RA, Mäkelä A, Reid DEB, Jokela EJ, Porté A, Roberts SD. 2010. Self-shading affects allometric scaling in trees. *Functional Ecology* 24: 723–730.
- Falster DS, Brännström Å, Dieckmann U, Westoby M. 2011. Influence of four major plant traits on average height, leaf-area cover, net primary productivity, and biomass density in single-species forests: a theoretical investigation. *Journal of Ecology* 99: 148–164.
- Falster DS, Westoby M. 2003. Leaf size and angle vary widely across species: what consequences for light interception? *New Phytologist* 158: 509–525.
- Farque L, Sinoquet H, Colin F. 2001. Canopy structure and light interception in *Quercus petraea* seedlings in relation to light regime and plant density. *Tree Physiology* 21: 1257–1267.
- Gálvez D, Percy RW. 2003. Petiole twisting in the crowns of *Psychotria limonensis*: implications for light interception and daily carbon gain. *Oecologia* 135: 22–29.
- Hallé F, Oldeman RAA, Tomlinson PB. 1978. *Tropical trees and forests: an architectural analysis*. Heidelberg, Germany: Springer-Verlag.
- Jackson JE, Palmer JW. 1979. A simple model of light transmission and interception by discontinuous canopies. *Annals of Botany* 44: 381–383.
- Kucharik CJ, Norman JM, Gower ST. 1999. Characterization of radiation regimes in nonrandom forest canopies: theory, measurements, and a simplified modeling approach. *Tree Physiology* 19: 695–706.
- Küppers M. 1989. Ecological significance of above-ground architectural patterns in woody plants: a question of cost-benefit relationships. *Trends in Ecology & Evolution* 4: 375–379.
- Kvålseth TO. 1985. Cautionary note about  $R^2$ . *The American Statistician* 39: 279–285.
- Lang ARG. 1991. Application of some of Cauchy's theorems to estimation of surface-areas of leaves, needles and branches of plants, and light transmittance. *Agricultural and Forest Meteorology* 55: 191–212.
- Lusk CH, Falster DS, Perez-Millaqueo MM, Saldana A. 2006. Ontogenetic variation in light interception, self-shading and biomass distribution of seedlings of the conifer *Araucaria araucana* (Molina) K. Koch. *Revista Chilena de Historia Natural* 79: 321–328.
- Lusk CH, Pérez-Millaqueo MM, Piper FI, Saldana A. 2011. Ontogeny, understory light interception and simulated carbon gain of juvenile rainforest evergreens differing in shade tolerance. *Annals of Botany* 108: 419–428.
- Mäkelä A. 1997. A carbon balance model of growth and self-pruning in trees based on structural relationships. *Forest Science* 43: 7–24.
- Mäkelä A, Sievänen R. 1992. Height growth strategies in open-grown trees. *Journal of Theoretical Biology* 159: 443–467.
- Massonnet C, Regnard JL, Lauri PÉ, Costes E, Sinoquet H. 2008. Contributions of foliage distribution and leaf functions to light interception, transpiration and photosynthetic capacities in two apple cultivars at branch and tree scales. *Tree Physiology* 28: 665–678.
- Monsi M, Saeki T. 1953. Über den Lichtfaktor in den Pflanzengesellschaften und seine Bedeutung für die Stoffproduktion. *Japanese Journal of Botany* 14: 22–52.
- Monsi M, Saeki T. 2005. On the factor light in plant communities and its importance for matter production. *Annals of Botany* 95: 549–567.
- Monteith JL. 1977. Climate and the efficiency of crop production in Britain. *Philosophical Transactions of the Royal Society of London, Series B* 281: 277–294.
- Moorcroft PR, Hurtt GC, Pacala SW. 2001. A method for scaling vegetation dynamics: the ecosystem demography model (ED). *Ecological Monographs* 71: 557–586.
- Niinemetts Ü, Sparrow A, Cescatti A. 2005. Light capture efficiency decreases with increasing tree age and size in the southern hemisphere gymnosperm *Agathis australis*. *Trees – Structure and Function* 19: 177–190.
- Nilson T. 1971. A theoretical analysis of the frequency of gaps in plant stands. *Agricultural Meteorology* 8: 25–38.
- Nilson T. 1999. Inversion of gap frequency data in forest stands. *Agricultural and Forest Meteorology* 98–99: 437–448.
- Ni-Meister W, Yang W, Kiang NY. 2010. A clumped-foliage canopy radiative transfer model for a global dynamic terrestrial ecosystem model. I: theory. *Agricultural and Forest Meteorology* 150: 881–894.
- Oker-Blom P, Smolander H. 1988. The ratio of shoot silhouette area to total needle area in Scots pine. *Forest Science* 34: 894–906.
- Percy RW, Duursma RA, Falster DS, PrometheusWiki contributors. 2011. *Studying plant architecture with Y-plant and 3D digitising*. PrometheusWiki. [WWW document] URL : <http://prometheuswiki.publish.csiro.au/tiki-index.php?page=Studying+plant+architecture+with+Y-plant+and+3D+digitising> [accessed on 26 September 2011].
- Percy RW, Muraoka H, Valladares F. 2005. Crown architecture in sun and shade environments: assessing function and trade-offs with a three-dimensional simulation model. *New Phytologist* 166: 791–800.
- Percy RW, Valladares F, Wright SJ, de Paulis EL. 2004. A functional analysis of the crown architecture of tropical forest *Psychotria* species: do species vary in light capture efficiency and consequently in carbon gain and growth? *Oecologia* 139: 163–177.
- Percy RW, Yang W. 1996. A three-dimensional crown architecture model for assessment of light capture and carbon gain by understory plants. *Oecologia* 108: 1–12.
- Planchais I, Sinoquet H. 1998. Foliage determinants of light interception in sunny and shaded branches of *Fagus sylvatica* (L.). *Agricultural and Forest Meteorology* 89: 241–253.
- R Development Core Team. 2010. *R: a language and environment for statistical computing*. Vienna, Austria: R Foundation for Statistical Computing. URL <http://www.R-project.org>.
- Reich P, Falster D, Ellsworth D, Wright I, Westoby M, Oleksyn J, Lee T. 2009. Controls on declining carbon balance with leaf age among 10 woody species in Australian woodland: do leaves have zero daily net carbon balances when they die? *New Phytologist* 183: 153–166.

- Roderick ML, Farquhar GD, Berry SL, Noble IR. 2001. On the direct effect of clouds and atmospheric particles on the productivity and structure of vegetation. *Oecologia* 129: 21–30.
- Ross J. 1981. *The radiation regime and architecture of plant stands*. The Hague, the Netherlands: Dr W. Junk.
- Sinoquet H, Sonohat G, Phattaralerphong J, Godin C. 2005. Foliage randomness and light interception in 3-D digitized trees: an analysis from multiscale discretization of the canopy. *Plant, Cell & Environment* 28: 1158–1170.
- Sinoquet H, Stephan J, Sonohat G, Lauri PE, Monney P. 2007. Simple equations to estimate light interception by isolated trees from canopy structure features: assessment with three-dimensional digitized apple trees. *New Phytologist* 175: 94–106.
- Stenberg P. 1996. Correcting LAI-2000 estimates for the clumping of needles in shoots of conifers. *Agricultural and Forest Meteorology* 79: 1–8.
- Stenberg P. 1998. Implications of shoot structure on the rate of photosynthesis at different levels in a coniferous canopy using a model incorporating grouping and penumbra. *Functional Ecology* 12: 82–91.
- Stenberg P. 2006. A note on the *G*-function for needle leaf canopies. *Agricultural and Forest Meteorology* 136: 76–79.
- Sterck FJ, Schieving F. 2007. 3-D growth patterns of trees: effects of carbon economy, meristem activity, and selection. *Ecological Monographs* 77: 405–420.
- Takenaka A. 1994. Effects of leaf blade narrowness and petiole length on the light capture efficiency of a shoot. *Ecological Research* 9: 109–114.
- Valentine HT, Mäkelä A. 2005. Bridging process-based and empirical approaches to modeling tree growth. *Tree Physiology* 25: 769–779.
- Valiente-Banuet A, Verdú M, Valladares F, García-Fayos P. 2010. Functional and evolutionary correlations of steep leaf angles in the mexican shrubland. *Oecologia* 163: 25–33.
- Valladares F, Dobarro I, Sánchez-Gómez D, Pearcy RW. 2005. Photoinhibition and drought in Mediterranean woody saplings: scaling effects and interactions in sun and shade phenotypes. *Journal of Experimental Botany* 56: 483–494.
- Valladares F, Niinemets Ü. 2007. The architecture of plant crowns: from design rules to light capture and performance. In: Pugnaire F, Valladares F, eds. *Functional plant ecology*. New York, NY, USA: Taylor and Francis, 101–149.
- Valladares F, Pearcy RW. 1998. The functional ecology of shoot architecture in sun and shade plants of *Heteromeles arbutifolia* M. Roem., a Californian chaparral shrub. *Oecologia* 114: 1–10.
- Valladares F, Pearcy RW. 1999. The geometry of light interception by shoots of *Heteromeles arbutifolia*: morphological and physiological consequences for individual leaves. *Oecologia* 121: 171–182.
- Valladares F, Skillman JB, Pearcy RW. 2002. Convergence in light capture efficiencies among tropical forest understory plants with contrasting crown architectures: a case of morphological compensation. *American Journal of Botany* 89: 1275.
- Valladares F, Wright SJ, Lasso E, Kitajima K, Pearcy RW. 2000. Plastic phenotypic response to light of 16 congeneric shrubs from a Panamanian rainforest. *Ecology* 81: 1925–1936.
- Vos J, Evers JB, Buck-Sorlin GH, Andrieu B, Chelle M, de Visser PHB. 2010. Functional-structural plant modelling: a new versatile tool in crop science. *Journal of Experimental Botany* 61: 2101–2115.
- Warton DI, Wright IJ, Falster DS, Westoby M. 2006. Bivariate line-fitting methods for allometry. *Biological Reviews* 81: 259–291.
- Whitehead D, Grace JC, Godfrey MJS. 1990. Architectural distribution of foliage in individual *Pinus radiata* D. Don crowns and the effects of clumping on radiation interception. *Tree Physiology* 7: 135–155.

## Supporting Information

Additional supporting information may be found in the online version of this article.

**Fig. S1** Residual analyses.

**Fig. S2** Analysis of residuals by taxonomic family.

**Table S1** Description of sources for the virtual plant database

**Methods S1** Scaling to the canopy level.

Please note: Wiley-Blackwell are not responsible for the content or functionality of any supporting information supplied by the authors. Any queries (other than missing material) should be directed to the *New Phytologist* Central Office.